Femtosecond Time-Resolved Hydrogen-Atom Elimination from Photoexcited Pyrrole Molecules

H. Lippert,[a] H.-H. Ritze,[a] I. V. Hertel,[a, b] and W. Radloff*[a]

Introduction

In recent years, the understanding of the photochemical processes in biologically relevant molecules in the gas phase has gained broad interest. In particular, aromatic biomolecules with an OH (hydroxy) or an NH (azine) group such as phenol, indole, pyrrole, or adenine were studied in detail. These molecules are important building blocks of naturally abundant compounds, such as proteins, porphyrins, or nucleic acids. As ab initio electronic-structure calculations and spectroscopic investigations suggested (see, e.g., ref. [1]), the key role of the photophysics in such molecules is played by an excited $\pi\sigma^*$ singlet state, which is characterized by a repulsive potential curve with respect to the O–H or N–H stretching coordinate. Generally, the dark $\pi\sigma^*$ state is not excited directly but is populated through neighboring $\pi\pi^*$ states. The coupling between the initially excited $\pi\pi^*$ state and the $\pi\sigma^*$ state, as well as the shape of the conical intersection of the $\pi\sigma^*$ state with the electronic ground state upon elongation of the X–H bond (X=O,N), determines the dynamics and energetics of the photochemical processes in these molecules.

The existence and properties of the repulsive $\pi\sigma^*$ state were demonstrated recently for different biomolecular systems, for example, for indole—the chromophore of the amino acid tryptophan—and its derivatives, on the basis of spectroscopic measurements.[2] The H-atom transfer reactions in phenol(NH$_3$)$_n$[3, 4] or indole(NH$_3$)$_n$ clusters,[5, 6] which were studied experimentally and theoretically, have also been interpreted on the basis of the $\pi\sigma^*$ state. The transfer of the H atom (from the OH group in phenol or the NH group in indole) to the NH$_3$ molecules of the cluster proceeds on the $\pi\sigma^*$ potential surface. The detection of neutral (NH$_3$)$_{n-1}$NH$_4$ radicals proves that a H-transfer reaction, followed by fragmentation, occurs.

However, until very recently, it was not clear whether the repulsive state could be confirmed only indirectly (for example, by the detection of the reaction products) or whether the H-atom elimination could also be observed directly. The experiments reported by the group of F. Temps[7] demonstrated, for the first time, the H-atom detachment from pyrrole in the excited $\pi\sigma^*$ state using photofragment velocity map imaging.

[a] H. Lippert, Dr. H.-H. Ritze, Prof. Dr. I. V. Hertel, Prof. Dr. W. Radloff
Max Born Institute, Max-Born-Straße 2A
12489 Berlin (Germany)
Fax: (+49)30-6392-1259
E-mail: radloff@mbi-berlin.de

[b] Prof. Dr. I. V. Hertel
Freie Universität Berlin, Physics Department
Arnimallee 14, 14195 Berlin (Germany)

Pyrrole is the photoreactive center of indole and represents one of the simplest heterocyclic aromatic ring molecules with a π-electron system. The lowest electronic state (at around 240 nm) has been assigned to the $1^1A_2(3s)$ Rydberg state,[8] which has, according to the calculations performed by Sobolewski and Domcke,[9, 10] a $\pi\sigma^*$ character due to a Rydberg-to-valence transformation. The antibonding σ^* orbital is located on the N–H bond, which leads to a repulsive potential with respect to the N–H coordinate. As the transition from the ground state to the $1^1A_2(\pi\sigma^*)$ state is electric-dipole-forbidden, its excitation around 240 nm is only possible by vibronic coupling with the nearby $\pi\pi^*$ states (2^1A_1 or 1^1B_2) induced by out-of-plane vibrations.[8] This behavior represents a Herzberg–Teller coupling similar to that observed, for example, in the $\tilde{A}^1B_{2u} \leftarrow \tilde{X}^1A_{1g}$ system of benzene.[11] At larger N–H distances the $\pi\sigma^*$ state of pyrrole crosses the electronic ground state by a symmetry-allowed conical intersection.[9] This leads to an ultrafast internal conversion to the ground state and should be the reason for the missing fluorescence of pyrrole in this wavelength region.

In the one-color experiments of Wei et al.[7] at 243.1 nm the photodissociation of the pyrrole molecule is initiated by a one-photon excitation, whereas the produced H atoms are detected by (2+1) resonance-enhanced multiphoton ionization (REMPI) spectroscopy. The authors found a dominant contribution ($\approx 76\%$) of fast H atoms with a narrow kinetic-energy distribution, which was assigned to a rapid, direct N–H bond dissociation, in agreement with the repulsive character of the excited $\pi\sigma^*$ state. This observation was also confirmed by the corresponding anisotropy parameter indicating the vibronic coupling between $\pi\pi^*$ and $\pi\sigma^*$. The second contribution is characterized by H atoms that exhibit a broad kinetic-energy distribution with a maximum at smaller velocities. This contribution is attributed to the fragmentation of the molecule in the electronic ground state after an internal conversion. Replacing the H atom of the NH group in pyrrole by a methyl group leads to the disappearance of the fast component; these results confirm that the fast component is, in fact, due to the direct dissociation of pyrrole in the $\pi\sigma^*$ state along the N–H bond. Quite similar conclusions were drawn in a previous study performed using photofragment translational spectroscopy,[12] where three dissociation channels were observed at 248 nm. Each channel involved a H-atom elimination. The dissociation from an excited electronic state ($\approx 47\%$) and the N–H bond cleavage after an internal conversion to the ground state ($\approx 42\%$) are the main contributions. The third channel ($\approx 11\%$) was attributed to a C–H bond cleavage in the excited electronic state.

In the present work we report on the results of a two-color pump–probe experiment with femtosecond laser pulses. The pyrrole molecules were excited at 250 nm and the products were probed by (2+1) REMPI at 243.1 nm. We were indeed able to detect H atoms using a femtosecond laser, despite the inefficient excitation of a narrow atomic resonance with the spectrally broad laser pulse. Thus, we were able to observe an ultrafast H-atom elimination on the excited $\pi\sigma^*$ state of a biomolecule directly for the first time. The analysis of the time-dependent H$^+$ signal reveals two time constants ($\tau_1 \approx 0.1$ ps, $\tau_2 \approx$

1.1 ps) for two subsequent H-atom formation channels, which seem to be correlated with the two contributions of the signals that were measured in the nanosecond experiments of Temps et al.[7]

Experimental Results

Figure 1 shows one-color time-of-flight (tof) mass spectra, which were obtained by photoionization of pyrrole at 250 nm and 243.1 nm. Each spectrum represents the average over $2\times$
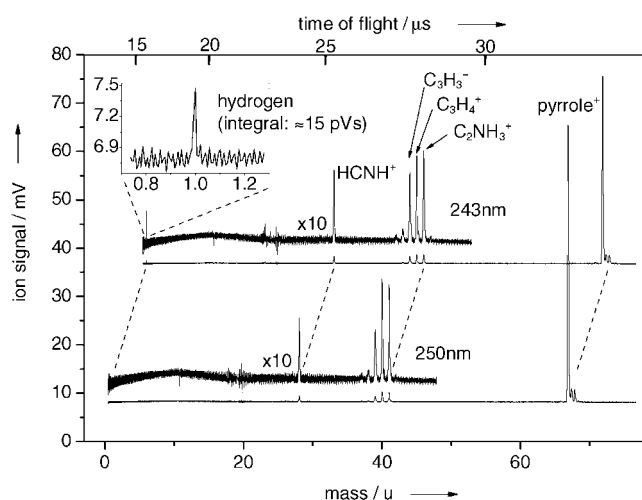
Figure 1. One-color mass spectra measured with femtosecond laser pulses at $\lambda = 250$ nm (bottom) and $\lambda = 243.1$ nm (top) alone. The laser intensities were comparable ($6–7 \times 10^{11}$ W cm^{-2}). The assignment of the mass peaks is based on ref. [15]. The hydrogen peak, which appears exclusively for 243.1 nm, can be clearly seen.

10^4 laser shots. The stronger 243.1 nm pulses were attenuated in such a way that comparable laser intensities at both wavelengths were obtained ($6–7 \times 10^{11}$ W cm^{-2}). Besides the prominent pyrrole$^+$ peak at $m/z = 67$ (observed in both spectra), the typical fragment ions at $m/z = 28$ and in the range $m/z = 37–41$ can also be seen. The formation of these ions was studied in detail previously.[13,14] The corresponding appearance energies lie above 12 eV so that in our case at least three photons are absorbed, possibly via a $(1+2)$ resonance-enhanced multiphoton ionization. When comparing the two mass spectra the most striking feature is the H$^+$ peak at $m/z = 1$, which is missing at 250 nm but is clearly recognizable at 243.1 nm. The appearance energy for the H$^+$ fragment ions in the pyrrole mass spectra is 17.71 eV,[14] which corresponds to the absorption of at least four photons. As this channel does not exist at 250 nm, it is evident that the $m/z = 1$ peak at 243.1 nm can only be caused by neutral H atoms, which are selectively detected via $(2+1)$ REMPI by the femtosecond laser pulses. Whether the hydrogen atoms originate from ion fragmentation or from fragmentation in the excited state will be discussed below.

Figure 2 shows time-dependent ion signals that were obtained at different mass channels. The Xe$^+$ signal in Figure 2c resembles a step function that can be explained by a two-
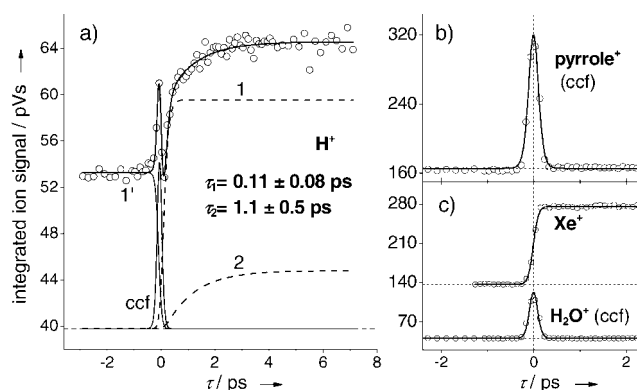
Figure 2. Ion signals of H$^+$, pyrrole$^+$, Xe$^+$, and H$_2$O$^+$ as a function of the delay time τ between pump (250 nm) and probe (243.1 nm) pulses. For H$^+$ the solid fit curve (——) is a superposition of different contributions (-----) revealing the time constants τ_1 and τ_2.

photon excitation of a long-lived atomic state at 250 nm followed by ionization at 243.1 nm (see Experimental Section). Figure 2c also shows the H$_2$O$^+$ ion transient, which, at these wavelengths, originates from a nonresonant three-photon ionization. This transient was fitted by a second-order cross-correlation-type function (ccf), from which a pulse length of 160 fs was derived. This value was also verified in independent measurements (not shown here) by comparison with the nonresonant signal that results from krypton ions. Therefore, the H$_2$O$^+$ signal may be used to determine the zero delay time between pump and probe pulses. Interestingly, the time-dependent pyrrole$^+$ signal shown in Figure 2b also reveals, mainly, a nonresonant contribution without showing any dynamics. This will be discussed in more detail in the next section.

Figure 2a shows the rather unusual transient obtained on the hydrogen-ion mass channel. The curve displays a quite asymmetric shape, which (considering the similarity of the wavelengths chosen) already indicates that a highly resonant process is involved. While the signal for $\tau < 0$ is flat, there is a steep increase for positive delay times. After ≈ 6 ps a plateau is reached. At $\tau = 0$ we observe a peak that shows a cross-correlation-type behavior. Beyond that, three main contributions have to be accounted for: The fit for $\tau > 0$ clearly reveals two distinct time constants in the sub-picosecond and picosecond ranges. In addition, a constant two-color pump–probe signal is observed also for $\tau < 0$ (i.e., where $\lambda_{pu} = 243.1$ nm and $\lambda_{pr} = 250$ nm). These results could easily be checked by comparison with the corresponding one-color background contributions. In the following, we will give a reasonable interpretation of our findings.

Discussion

As described in the Experimental Section, the pump and probe laser beams were strongly focused to guarantee a sufficiently high ionization efficiency for the H atoms by three-probe photon absorption. Hence, we did not only observe the pump–probe signal of interest but also several "background" contributions due to the multiphoton absorption of the pyrrole molecule and the neutral hydrogen fragments.

We will start by discussing the different mass spectra obtained by the one-color irradiation of pyrrole, that is, the ionization by pump or probe pulse only (Figure 1). For $\lambda = 243.1$ nm we observed a significant H^+ signal whereas for $\lambda = 250$ nm this signal was not detected. As mentioned, the one-photon excitation of the 0_0^0 band of the $1^1A_2(\pi\sigma^*)$ state is symmetry-forbidden. However, at the central wavelengths of our femtosecond pulses (250 and 243.1 nm), it is possible to excite higher vibrational bands of the $\pi\sigma^*$ state directly via a Herzberg–Teller coupling.[8] There are several vibronic transitions involving modes of b_1 or a_2 symmetry that "borrow" intensity from the energetically higher $1^1B_2(\pi\pi^*)\leftarrow S_0$ or $1^1A_1(\pi\pi^*)\leftarrow S_0$ transitions. Therefore, at both wavelengths, the resonant one-photon absorption leads to an excitation of the $\pi\sigma^*$ state, which is repulsive with respect to the N–H bond (see Introduction). The pyrrole molecules dissociate on an ultrafast timescale yielding neutral H atoms as fragments. At 243.1 nm these fragments are ionized within the pulse duration, while at 250 nm ionization is not possible due to the energetic mismatch with the transition $2^2S \leftarrow 1^2S$. Figure 3a illustrates the process descri-
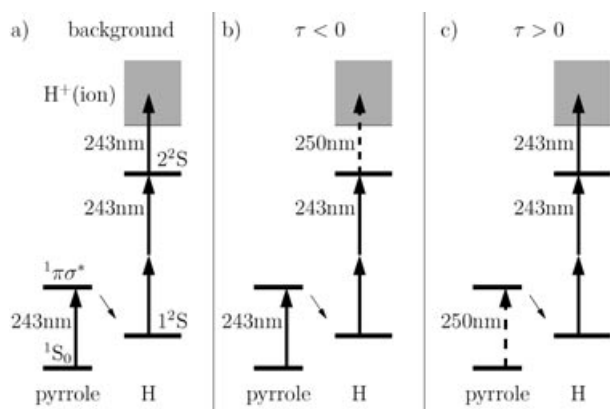
Figure 3. The formation paths for H^+ that contribute to the time-dependent ion signal shown in Figure 2a.

bed. The fact that the H^+ signal at 243.1 nm is so weak can be explained by the low efficiency of the $(2+1)$ multiphoton ionization, as well as by the small oscillator strengths of the $\pi\sigma^*$ vibronic transitions.[8]

It is worth noting that the H atoms originate solely from the repulsive excited state of pyrrole and not from ion fragmentation. In principle, one could think of two relevant channels:[14] one corresponds to the direct dissociation of pyrrole cations giving a mass peak at $m/z = 66$ ($C_4H_5N^+ \rightarrow C_4H_4N^+ + H$); although this channel is energetically accessible (appearance energy: 13.05 eV[14]), it cannot be important since we observe practically no signal at $m/z = 66$ as can be seen in Figure 1. The second channel ($C_4H_5N^+ \rightarrow C_2H_2N^+ + C_2H_2 + H$) could, in principle, contribute to the signal at $m/z = 40$ (which corresponds to $C_3H_4^+$). However, this process has a threshold of 16.5 eV and, hence, since it demands more than three photons, it can also be excluded. We can state that the prominent pyrrole fragment peaks in the mass spectra arise solely from well-defined

ion fragmentation reactions,[13,14] which do not involve hydrogen formation. Another corroborative argument is based on the fact that such a hypothetical formation event would have to take place on an ultrashort time scale, since formation and H-atom ionization both occur within one laser pulse. Consequently, one would expect a repulsive ion state, which is unlikely in this case. The same argumentation is valid to rule out highly excited pyrrole Rydberg states that might be conceivable.

We will now discuss the pump–probe transients shown in Figure 2a. It is obvious that the one-color H^+ signal at 243.1 nm (Fig. 3a) represents the background signal on the hydrogen mass channel. In the same way, we obtain a constant signal for $\tau < 0$, which arises from the interplay of the two pulses as indicated in Figure 3b. With a "pump" wavelength of 243.1 nm, neutral H atoms are formed, a part of which is excited resonantly to the 2^2S electronic state by the absorption of two additional photons during the pulse; the time-delayed "probe" photon at 250 nm then ionizes the excited H atoms giving a constant signal contribution for $\tau < 0$. Finally, Figure 3c illustrates the "real" pump–probe process at $\tau > 0$: the neutral H atoms are formed after exciting the pyrrole molecule with $\lambda_{pu} = 250$ nm; after a delay time τ they are then detected by $(2+1)$ photons of $\lambda_{pr} = 243.1$ nm.

In Figure 2a, the constant H^+ signal for $\tau < 0$ is clearly displayed (contribution 1'). The narrow signal peak at $\tau = 0$ was considered in the fitting procedure by including a cross correlation contribution due to the simultaneous absorption of pump and probe photons. The time-dependent H^+ signal of interest for $\tau > 0$ obviously represents the superposition of two rising signals with the time constants τ_1 and τ_2. The values for these time constants were determined by fitting the experimental points to a theoretical curve according to our model. We were able to resolve a very fast signal rise with a time constant $\tau_1 = 0.11 \pm 0.08$ ps. This process is followed by a somewhat slower rise of the H^+ signal with the time constant $\tau_2 = 1.1 \pm 0.5$ ps. The large errors are caused by the finite accuracy of the experimental data and, in particular, by the uncertainty of the fitting procedure. The latter can mainly be explained by the fact that we are dealing with a sharp atomic resonance and non-bandwidth-limited pulses, which do not allow for an exact determination of the zero delay time. Furthermore, the extremely large error of τ_1 can also be ascribed to the limited time resolution of our experiments.

The interpretation of the observed dynamics of the H-atom elimination after the photoexcitation of pyrrole is based on the potential-energy scheme represented in Figure 4. This scheme is adapted to the corresponding potential curves calculated with respect to the N–H coordinate of pyrrole by Sobolewski and Domcke.[9] Only the lowest $^1\pi\pi^*$ and $^1\pi\sigma^*$ states, as well as the electronic ground state, are indicated. The most important feature is the symmetry-allowed crossing of the repulsive $\pi\sigma^*$ state with the S_0 ground state. In a multidimensional picture, these states form a conical intersection through which the internal conversion to the ground state can occur if nonadiabatic coupling by other vibrational modes is taken into account. The corresponding double cone, which shows up upon displace-
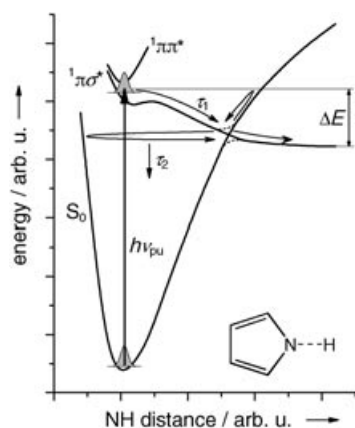
Figure 4. Schematic representation of the potential-energy curves and possible wave-packet dynamics of pyrrole as a function of the N–H stretching coordinate. The curves correspond to those calculated by Sobolewski and Domcke.[9] The $\pi\pi^*$ and $\pi\sigma^*$ states are Herzberg–Teller coupled via nontotally symmetric modes. The double cone that appears where the $\pi\sigma^*$ surface crosses the S_0 surface is indicated by the dashed lines. τ_2 is related to a vibrational redistribution in the ground state.

ment along these modes, is indicated in the graph (dashed lines in Figure 4).

As described, the $\pi\sigma^*$ state is populated via intensity "borrowing" from the $\pi \rightarrow \pi^*$ transitions. The latter are off-resonant (≥ 0.5 eV[8]) and a corresponding $\pi\pi^*$ population can be neglected. Therefore, we can safely assume that, by absorbing the pump photon $h\nu_{pu}$ at 250 nm, a wave packet is directly excited on the repulsive $\pi\sigma^*$ state of the pyrrole. This packet propagates on the $\pi\sigma^*$ potential curve as shown in Figure 4. The movement corresponds to a collapse of the antibonding σ^* orbital towards the $1s$ orbital of hydrogen (Rydberg-to-valence transition) and will partially lead to a *direct* dissociation of H atoms with the time constant τ_1. The available energy ΔE is converted almost completely into kinetic energy, which is essentially carried away by the light H atom. This would lead to a relatively narrow distribution of the kinetic energies. The rather large value of $\tau_1 \approx 0.1$ ps might be caused by the shallow barrier that separates the inner Rydberg part of the potential-energy function from its outer valence part (see Fig. 4 and ref. [9]).

The time constant τ_2 is linked to an *indirect* dissociation process. When the propagating wave packet passes the conical intersection (after τ_1), there is a certain probability that vibrationally highly excited pyrrole molecules in the electronic ground state emerge. Here a fragmentation by H-atom elimination is possible as long as the vibrational energy in the N–H mode is above the dissociation threshold given by the lower dashed line in Figure 4. In a sense, the dissociation process itself is associated with a subsequent internal conversion back to the $\pi\sigma^*$ state. Several vibrational redistribution processes may lead to a decay of the energy stored in the N–H mode and thus cause a limitation of the H-atom formation with the time constant τ_2. In this case, the kinetic energy of the H atoms is expected to be broadly distributed over the whole energy range (ΔE having a maximum at somewhat smaller en-

ergies due to the internal vibrational cooling). Whether (and to what extent) the indirect dissociation is based on the proposed mechanism, could presumably be revealed by quantum dynamics calculations.

By comparing our results with those of Temps et al.[7] it is suggested that the contribution of H atoms formed directly with the time constant τ_1 represents the fraction of fast fragments reported there. The contribution of H atoms formed within a longer time (τ_2) should then correspond to the broad distribution of slower H atoms detected by Temps. A ratio of about three was reported for both contributions, which roughly agrees with the weights of the components with τ_1 and τ_2 found in our experiments (cf. dashed lines in Figure 2a). It should be noted, however, that further potential fragmentation channels on the nanosecond time scale cannot be observed in our experiments.

Finally, we have to discuss the time-dependent signal of the parent ion (see Figure 2b). The measured signal can be fitted by a cross correlation function (ccf), which is similar to the nonresonant H_2O^+ signal. This means that for both wavelengths, that is, for 250 nm at $\tau > 0$ and for 243.1 nm at $\tau < 0$, the decay of the excited pyrrole state is extremely fast and, thus, cannot be observed with respect to the relatively broad cross correlation signal. The ultrafast propagation of the wave packet on the repulsive $\pi\sigma^*$ state surface, which reflects the rapid stretch of the N–H bond, leads to molecular geometries that (for Franck–Condon reasons) cannot be ionized by the probe photons. Furthermore, one might, in principle, expect to be able to trace the dynamics found for hydrogen also on the corresponding pyrrolyl radical mass channel. This was not possible in our experiments. Presumably, the detection efficiency for C_4H_4N was too low due to a rather high ionization potential and a poor Franck–Condon overlap.

Conclusions

For the first time we have detected neutral hydrogen atoms via (2+1) resonance-enhanced multiphoton ionization by femtosecond laser pulses at 243.1 nm. This technique enabled us to trace directly (in a pump–probe setup) the H-atom detachment in pyrrole after photoexcitation at 250 nm. We observed a fast time constant of $\tau_1 \approx 0.1$ ps, which agrees well with a model including a $\pi\sigma^*$ state that is repulsive along the N–H coordinate and shows a conical intersection with the electronic ground state.[9, 10] A second time constant (of $\tau_2 = 1.1 \pm 0.5$ ps) indicates an indirect dissociation mechanism that may be explained by an internal vibrational cooling in the electronic ground state, which is populated after an internal conversion (due to a nonadiabatic coupling with the first excited electronic state) has occurred. The results can be directly compared with those obtained from nanosecond experiments[7] where two different channels were found with respect to the kinetic energy of the hydrogen fragments.

For future experiments it will be very interesting to check whether and on which time scale the H-atom abstraction occurs as a photochemical process in larger molecules such as nucleobases. This would shine further light onto the general

microscopic mechanisms that are discussed in the context of the nonradiative decay in aromatic biomolecules.

Experimental Section

By vaporizing pyrrole into an evacuated gas reservoir and subsequent filling with He seed gas and small amounts of Xe, we prepared a gas mixture that contained 0.1–0.2% of pyrrole. At a backing pressure of 1 bar the mixture was adiabatically expanded into our molecular-beam apparatus through a pulsed piezo nozzle operating at 350 Hz. After passing through a 1 mm skimmer, the molecular beam entered the interaction region of a Wiley–McLaren time-of-flight mass spectrometer where it was crossed by two strongly focused non-collinear laser beams. In the experiments we usually observed a certain amount of water emerging as a background signal.

The laser beams were generated by a commercial (Spectra Physics GmbH) Ti: sapphire oscillator (TSUNAMI) and amplifier (SPITFIRE) fs laser system. Two optical paramatric generator/amplifier devices (TOPAS model 4/800/f, light conversion) allowed for a tunable wavelength selection in the pump–probe experiments. For both pump and probe pulses we used the second harmonic of the output of each TOPAS system generated by sum-frequency mixing of the signal (1333 and 1239 nm) and the fundamental (800 nm) pulses. Typically, the laser fluence of the pump pulse at $\lambda_{pu} = 250$ nm (4.96 eV) was around 90 mJ cm^{-2}, which corresponds to a peak intensity of $\approx 6 \times 10^{11}$ W cm^{-2}, while for the probe pulse at $\lambda_{pr} = 243.1$ nm (5.1 eV) it was ≈ 160 mJ cm^{-2} (ca. 10^{12} W cm^{-2}). The specific probe wavelength of 243.1 nm was chosen to detect neutral H atoms by (2+1) REMPI via the Lyman-α transition. The temporal width of the laser pulses was about 160 fs. The pulses were not bandwidth-limited.

A standard translation stage was used to scan the time delay between pump and probe pulses. In order to find their spatial and temporal overlap, we took advantage of the long-lived $5p^5(^2P_{3/2})6p[1/2]_{J=0}$ xenon intermediate state,[15] which can normally be excited by a two-photon transition at 250 nm and ionized by one photon at 243.1 nm.

Typically, the mass spectra were accumulated for 200 laser shots at each time delay τ and averaged over 180 up- and down-scans of the delay line. We scanned over two different time ranges with a step size of 100 and 200 fs. For the analysis, both data sets have been combined.

[1] A. L. Sobolewski, W. Domcke, C. Dedonder-Lardeux, C. Jouvet, *Phys. Chem. Chem. Phys.* **2002**, *4*, 1093.
[2] B. C. Dian, A. Longarte, T. S. Zwier, *J. Chem. Phys.* **2003**, *118*, 2696.
[3] O. David, C. Dedonder-Lardeux, C. Jouvet, *Int. Rev. Phys. Chem.* **2002**, *21*, 499.
[4] K. Daigoku, S. Ishiuchi, M. Sakai, M. Fujii, K. Hashimoto, *J. Chem. Phys.* **2003**, *119*, 5149.
[5] H. Lippert, V. Stert, L. Hesse, C. P. Schulz, I. V. Hertel, W. Radloff, *J. Phys. Chem. A* **2003**, *107*, 8239.
[6] H.-H. Ritze, H. Lippert, V. Stert, W. Radloff, I. V. Hertel, *J. Chem. Phys.* **2004**, *120*, 3619.
[7] J. Wei, A. Kuczmann, J. Riedel, F. Renth, F. Temps, *Phys. Chem. Chem. Phys.* **2003**, *5*, 315.
[8] B. O. Roos, P.-Å. Malmqvist, V. Molina, L. S. Serrano-Andrés, M. Merchán, *J. Chem. Phys.* **2002**, *116*, 7526.
[9] A. L. Sobolewski, W. Domcke, *Chem. Phys.* **2000**, *259*, 181.
[10] A. L. Sobolewski, W. Domcke, *Chem. Phys. Lett.* **2000**, *321*, 479.
[11] J. M. Hollas, *High resolution spectroscopy*, 2nd ed., John Wiley & Sons, Chichester, **1998**.
[12] D. A. Blank, S. W. North, Y. T. Lee, *Chem. Phys.* **1994**, *187*, 35.
[13] G. D. Willett, T. Baer, *J. Am. Chem. Soc.* **1980**, *102*, 6774.
[14] E. E. Rennie, C. A. F. Johnson, J. E. Parker, R. Ferguson, D. M. P. Holland, D. A. Shaw, *Chem. Phys.* **1999**, *250*, 217.
[15] C. E. Moore, *Atomic energy levels*, Vol *III*, US Gov. Printing Office, Washington DC, **1958**.